

1           **Compounding seasonal variations in outlet glacier**  
2           **dynamics revealed by high-resolution observations**

3           **Enze Zhang<sup>1</sup>, Ginny Catania<sup>1,2</sup>, Ben Smith<sup>3</sup>, Denis Felikson<sup>4</sup>, Beata Csatho<sup>5</sup>,**  
4           **and Daniel T. Trugman<sup>6</sup>**

5                           <sup>1</sup>The University of Texas at Austin, Institute of Geophysics, TX, USA

6                           <sup>2</sup>The University of Texas at Austin, Department of Geological Sciences, TX, USA

7                           <sup>3</sup>Polar Science Center, Applied Physics Laboratory, University of Washington, Seattle, WA, USA

8                           <sup>4</sup>Cryospheric Sciences Laboratory, NASA Goddard Space Flight Center, Greenbelt, MD, USA

9                           <sup>5</sup>Department of Geological Sciences, University at Buffalo, Buffalo, NY, USA

10                          <sup>6</sup>Nevada Seismological Laboratory, Nevada Geosciences, University of Nevada, Reno, NV, USA

11           **Key Points:**

- 12           • Simple model can be used to attribute a portion of seasonal velocity variability  
13           caused by terminus position change.
- 14           • Seasonal velocity variability is complex and results from multiple compounding  
15           processes.
- 16           • Seasonal velocities are more sensitive to surface slope changes than uniform changes  
17           in elevation.

---

Corresponding author: Enze Zhang, [zhangenze@link.cuhk.edu.hk](mailto:zhangenze@link.cuhk.edu.hk)

## Abstract

Understanding seasonality in outlet glacier dynamics reveals insight into long-term retreat and acceleration. Leveraging recent high-resolution satellite data, we examine changes in surface elevation, velocity, and terminus position for five glaciers in Central Western Greenland over the past  $\sim 6$  years. We employ an approach that examines the stress imbalance at the ice-ocean terminus and models the expected response in upstream velocity caused by the observed terminus changes. The model shows that some glaciers' seasonal velocity changes can be largely explained by terminus changes, while others can be compounded by multiple processes. Additionally, we test the sensitivity of the results by including seasonally varying and artificially modified surface topography. We find surface slope changes impact velocity response to terminus changes more than spatially uniform changes in along-flow elevation. Our approach provides a scalable framework to comprehend the compounded nature of glacier seasonal velocity variations across the Greenland Ice Sheet outlet glaciers.

## Plain Language Summary

Understanding seasonal changes in glaciers is crucial for studying long-term trends. To capture glacier seasonality in detail, we combine detailed data on glacier speed and terminus movement at sub-weekly to daily intervals, along with seasonal surface topography data. We use a model that reveals how much glacier speed changes in response to terminus variations. For some glaciers, our model shows that seasonal glacier speed change is completely driven by terminus change. For other glaciers, we find that seasonal velocity changes can be influenced by runoff and seasonal changes in the drainage system beneath the glacier, in addition to terminus position change. Additional tests suggest that change in the surface slope of a glacier has a stronger impact on the sensitivity of seasonal speed changes to terminus changes than uniform changes in glacier surface topography; flattening of the glacier surface results in less sensitivity of the surface velocity to terminus changes. Our approach provides a framework to expand these observations to the entire Greenland to reveal the complexity of glacier seasonality.

## 1 Introduction

The Greenland Ice Sheet (GrIS) is currently the largest land ice contributor to present-day rising sea level (IPCC, 2022) with an acceleration in mass loss over the past few decades primarily attributed to ice discharge through outlet glaciers (Shepherd et al., 2012; Enderlin et al., 2014; van den Broeke et al., 2016). This acceleration underscores the importance of comprehending the intricate mechanisms that govern glacier dynamics. Despite the prevalence of glacier acceleration in Greenland, there exists notable spatio-temporal variability in glacier velocity change at a range of time scales (Moon et al., 2012, 2020), which is likely influenced by local conditions, like topography, and regionally by environmental factors. For example, runoff and ocean thermal forcing can influence velocity by changing basal friction (Ultee et al., 2022), subaqueous melt rates (Holland et al., 2008), and through terminus fluctuations (Howat et al., 2008; King et al., 2020; Wood et al., 2021). At the seasonal scale, many of these processes are synchronized, making it difficult to understand the cause and effect behind seasonal glacier acceleration. Despite this, recent advances in the temporal frequency of satellite measurements provide an opportunity to examine the factors that force glacier dynamic change over multiple epochs (Kehrl et al., 2017). Moreover, numerical simulations suggest that glacier seasonal changes can induce systematic bias in mass loss estimates at the multi-decadal time scale (Felixson et al., 2022). Thus, delving into the patterns of glacier seasonality is instrumental in unveiling and simulating the pivotal factors that control glacier dynamics at longer time scales and into the future.

67           Glaciers across Greenland exhibit discernible seasonal changes in terminus posi-  
68           tion (Goliber et al., 2022; Catania et al., 2018; Zhang et al., 2023) and surface velocity  
69           (Moon et al., 2015; Joughin et al., 2008), but the mechanisms behind such changes are  
70           varied. Studies have suggested that seasonal glacier retreat due to summertime air tem-  
71           perature increases causes reduced contact with bed and/or fjord walls, which along with  
72           increased net force at the calving cliff, leading to glacier acceleration (Howat et al., 2005;  
73           Joughin et al., 2012). Others have indicated that glacier acceleration can be due to sea-  
74           sonal changes in basal lubrication related to changes in the subglacial hydrological sys-  
75           tem (Davison et al., 2020; Stevens et al., 2022; Werder et al., 2013; Andrews et al., 2014),  
76           which can cause complex responses from glacier velocities. Subglacial hydrology can be  
77           influenced by seasonal input of surface meltwater, which generates changes in basal wa-  
78           ter pressure that evolve over the summer as subglacial conduits grow more efficient (Andrews  
79           et al., 2014; Vijay et al., 2019). However, subglacial hydrology can also be influenced by  
80           remnant summer meltwater (Iken & Truffe, 1997), water storage englacially (Abe & Fu-  
81           ruya, 2015) and in basal crevasses (Harper et al., 2010), or exfiltrated groundwater (Robel  
82           et al., 2023), which can leak out of the subglacial system over time (Rennermalm et al.,  
83           2013).

84           Previous efforts have classified glacier seasonal velocity variations into types based  
85           on the observed timing of changes and correlation to runoff and terminus changes (Moon  
86           et al., 2014; Vijay et al., 2019, 2021). Three categories are generally described in the lit-  
87           erature; 1) positive correlation of glacier velocity to glacier terminus retreat; 2) positive  
88           correlation of glacier velocity to seasonal summer runoff, and; 3) glacier velocity that slows  
89           in late summer and speeds up in winter. Recently, Solgaard et al. (2022) applied a ma-  
90           chine learning approach to analyze velocity time series data across Greenland, reveal-  
91           ing similar seasonal patterns as those first identified by Moon et al. (2014), however both  
92           studies used data with limited sampling frequency, resulting in possible aliasing of sub-  
93           seasonal velocity changes. Here, we re-examine glacier seasonality using high-frequency  
94           terminus (Zhang et al., 2023) and velocity (Gardner et al., 2023) observations, within  
95           an analytical model of velocity response to terminus position change (Joughin et al., 2012),  
96           to explore how compounding processes influence glacier seasonality. Additionally, we in-  
97           tegrate a seasonally-varying elevation dataset into our analysis to assess the impact of  
98           elevation change on the seasonal velocity response of a glacier. By comparing model re-  
99           sults with observed velocity time series, our results indicate that sub-seasonal glacier ve-  
100          locity change can be caused by the interplay of multiple processes.

## 101   **2 Data, study regions, and method**

102          We investigate five glaciers in central-west Greenland (Figure 1): Rink Isbrae (RNK),  
103          Sermeq Avannarleq (AVA), Sermeq Kujalleq (KUJ), Kangilernata Sermia (KAN), and  
104          Eqip Sermia (EQP) over the time period 2015-2021. This time span is specifically cho-  
105          sen to take advantage of the increased sample frequency available in both velocity and  
106          terminus position data due to the launch of Sentinel-1/2 in 2014. These five glaciers are  
107          selected because 1) they exhibit regular seasonal changes in both terminus and veloc-  
108          ity changes (Catania et al., 2018; Fried et al., 2018) with minimal long-term variations  
109          over our study period and; 2) they exhibit a range of sub-seasonal behavior in both the  
110          terminus and velocity variability. For example, all glaciers advance in winter and retreat  
111          in summer and yet their seasonal velocity behavior differs over time and space. EQP and  
112          KUJ speed up during summertime terminus retreat while AVA and KAN slow down dur-  
113          ing summertime terminus retreat (Fried et al., 2018). AVA, KUJ, KAN, and EQP are  
114          located close to one another, suggesting that they likely experience the same regional cli-  
115          mate forcing. We also examine RNK, which is further north than these four glaciers be-  
116          cause it has a deep grounding line, in contrast to the shallower grounding lines of the  
117          other four glaciers to the south, and a partially floating terminus that permits large, buoy-

118 ant flexure-style calving events driving glacier-wide step changes in the terminus posi-  
 119 tion (Medrzycka et al., 2016; Fried et al., 2018).

120 We use dense velocity time series data generated using auto-RIFT (Gardner et al.,  
 121 2018) and provided by the NASA MEaSURES ITS\_LIVE project (Gardner et al., 2023).  
 122 ITS\_LIVE combines velocity products derived from Landsat-8, Sentinel-1, and Sentinel-  
 123 2 producing a near-daily temporal resolution since 2014. For each glacier, we identify  
 124 multiple flowlines across the glacier from Felikson et al. (2021) and extract velocities at  
 125 points that are situated roughly 1-2 kilometers upstream from the terminus along each  
 126 flowline. We then average these velocities across all flowlines to produce a mean veloc-  
 127 ity time series for each glacier. RNK has eight flowlines because half of the terminus re-  
 128 gion of this glacier is floating and we want to examine the velocity variations of the float-  
 129 ing and grounded ice separately. We identify floating ice based on the flattening of the  
 130 surface elevation along flowlines towards the terminus and we take the mean of the ve-  
 131 locities on floating ice and grounded ice separately (Figure S1). We refrain from employ-  
 132 ing bed elevation data to ascertain the floating condition for RNK because of the reliance  
 133 of the bed data on mass conservation and the assumption that the glacier is grounded,  
 134 as described below (Morlighem et al., 2017). Terminus position data come from AutoTerm  
 135 (Zhang et al., 2023), a machine learning pipeline that automatically produces terminus  
 136 traces with an average sampling frequency of 10 per month since 2014. We derive a time  
 137 series of terminus changes by calculating sequential area changes between termini, ac-  
 138 cumulating these over time, and then normalizing this by the glacier width.

139 Surface elevation data come from a novel fusion of ICESat-2 data with DigitalGlobe  
 140 high-resolution digital elevation models (DEM), termed “DG-IS2-DEM”. Four DEMs  
 141 per year are available since Fall 2018. We also use ArcticDEM (Porter et al., 2022) as  
 142 supplementary elevation data in locations where the DG-IS2-DEM does not extend to  
 143 the most advanced terminus position found in AutoTerm. To get ice thickness data, we  
 144 subtract surface elevation data from bed elevation data from BedMachineV5 (Morlighem  
 145 et al., 2022), which assimilates seafloor bathymetry and ice thickness data through a mass  
 146 conservation approach (Morlighem et al., 2017). We extract the surface and bed eleva-  
 147 tion profiles along each flowline individually. We use GSFC-FDMv1.2.1 simulations of  
 148 the surface mass balance (Medley et al., 2022) to produce a runoff time series with a five-  
 149 day sampling frequency. We use runoff as a proxy for the start and end of the melt sea-  
 150 son.

151 We adopt the terminus-driven model described by Joughin et al. (2012) to predict  
 152 the seasonal terminus velocity, which explicitly considers the influence of the dynamic  
 153 changes at the glacier terminus on upstream velocity. For each flowline, we employ its  
 154 associated geometry profile for velocity simulations. By using the terminus-driven model,  
 155 we are able to isolate the contribution of sub-annual terminus variations to the observed  
 156 variations in the velocity time series. The terminus-driven model focuses on the driv-  
 157 ing stress ( $\tau_d$ ) and an additional force due to the presence of the free calving face deter-  
 158 mined by the height above the fjord surface at the calving front and the density of sea-  
 159 water. The difference between these two forces at the terminus is expressed as

$$F = \frac{1}{2} \times \rho_i g H^2 - \frac{1}{2} \times \rho_w g (H - h)^2 \quad (1)$$

160 where  $g$  is the gravitational acceleration,  $H$  is ice thickness,  $h$  is ice surface elevation,  
 161  $\rho_w$  is the density of seawater ( $1028 \text{ km m}^{-3}$ ), and  $\rho_i$  is the density of ice ( $910 \text{ km m}^{-3}$ ).  
 162 The force balance at the terminus requires the frontal force,  $F$ , to be balanced upstream  
 163 by the longitudinal stress, which redistributes much of the frontal force to the margins  
 164 and bed of the glacier upstream. The longitudinal stress that originates from the frontal  
 165 force ( $\tau_F(x)$ ) pulls the glacier and enhances the original driving stress (e.g.,  $\tau_d + \tau_F(x)$ ).  
 166 The enhanced driving stress is considered to be balanced by resistance stress (e.g., basal  
 167 drag and lateral shear stress). Based on the observation that the seasonal amplitude of

168 velocity is strongest at the terminus and diminishes upstream, Joughin et al. (2012) made  
 169 the assumption that  $\tau_F(x)$  decreases linearly from the terminus to zero at the stress cou-  
 170 pling length, and the integration of  $\tau_F(x)$  along the flowline equals  $F$ .

171 By assuming a linear relationship between velocity and the cube of  $\tau_d + \tau_F(x)$  (Van der  
 172 Veen, 2013), the predicted velocity from terminus changes is thus given by:

$$\frac{V(x,t)}{V_0} = \left( \frac{\tau_d + \tau_F(x)}{\tau_d + \tau_{F_0}} \right)^3 \quad (2)$$

173 where  $V_0$  is a reference velocity and  $\tau_{F_0}$  is the  $\tau_F(x)$  for the reference velocity. The as-  
 174 sumption holds when resistance increases with glacier speed due to factors like increased  
 175 internal ice deformation (e.g., laminar flow) or larger basal friction over a rough and rigid  
 176 bed (Van der Veen, 2013). For each year, we use the minimum velocity as the reference  
 177 velocity and calculate  $\tau_{F_0}$  based on the terminus position near the date of the reference  
 178 velocity. We vary stress coupling lengths for each glacier and choose the one that pro-  
 179 duces the lowest mean difference between observations and simulated velocity (Table S1).  
 180 The mean difference is determined by:

$$\frac{\text{abs}(\text{model} - \text{observation})}{\text{model}} \times 100\% \quad (3)$$

181 Using Eqn. 2 we simulate a velocity time series at each observation point for each glacier  
 182 (Figure 1) and average the simulated velocity across all flowlines in a manner consistent  
 183 with observed velocity. Subsequently, we compare these averaged simulated velocities  
 184 to observed velocity.

185 We make use of the new time-varying DG-IS2-DEM in order to determine if sea-  
 186 sonal changes in surface elevation may also produce seasonal changes in velocity in ad-  
 187 dition to those driven by seasonal terminus change. To accomplish this, we produce a  
 188 simulated velocity for all glaciers with and without time-varying surface elevation. For  
 189 the fixed geometry simulations, we choose a time step from DG-IS2-DEM with an ext-  
 190 ent that aligns best with the position of the terminus when it is most advanced. This  
 191 provides the most complete elevation profile across the terminus region. For EQP, KAN,  
 192 and AVA we choose the October 2019 DG-IS2-DEM and for KUJ, we use the April 2019  
 193 DG-IS2-DEM time step. For RNK, we use additional elevation data from ArcticDEM  
 194 (Porter et al., 2022) for the fixed geometry case, as the DG-IS2-DEM does not cover the  
 195 most advanced terminus position for this glacier.

### 196 3 Results

197 We compare the simulated velocity time series with velocities from satellite obser-  
 198 vations to determine whether seasonal velocity variations are influenced primarily by ter-  
 199 minus change, co-influenced by other factors, or entirely independent of terminus change.  
 200 Overall, we find that the time-series velocity observations from 2015 are well-described  
 201 by the terminus-driven model for RNK, KUJ, and EQP but not for KAN and AVA (Fig-  
 202 ure 2, S2–S6). For RNK, KUJ, and EQP, seasonal changes in glacier speed align well with  
 203 terminus variations. This is supported by the coincident timing of the end of terminus  
 204 retreat and the peak summertime velocity (vertical black lines in Figure 2), even in in-  
 205 stances when retreat continues beyond the end of the melt season (Figure 21). For these  
 206 glaciers, the mean misfit between simulated and observed velocities over all years are 4.6%  
 207 for KUJ, 6.2% for EQP, and 6.8% for RNK (Table S1), with correlations of 0.84, 0.67,  
 208 and 0.56, respectively (Figure S7).

209 Although the terminus-driven model adequately resolves seasonal variability in ve-  
 210 locity for RNK, KUJ, and EQP, there are observed sub-seasonal velocity changes that  
 211 are not explained by the terminus-driven model. For all glaciers but KUJ, we observe

212 additional pulses in velocity (acceleration and deceleration) in the middle of the melt sea-  
 213 son, a phenomenon not captured by the terminus-driven model (black dashed boxes in  
 214 Figure 2l). While these are predominant, they do not occur consistently across all years  
 215 for all glaciers. For example, melt-season pulses are visible for every year in the record  
 216 for AVA (Figure S3) but they are only visible from 2015-2019 for KAN (Figure S5), from  
 217 2016-2019 for EQP (Figure S6), and in 2015, 2017, and 2019 for RNK (Figure S2).

218 In addition to melt-season velocity pulses, we find additional sub-seasonal pulses  
 219 that coincide with large calving events. Such events are only visible on RNK, which ex-  
 220periences much larger calving events than the other glaciers and are associated with step  
 221 changes in the terminus position. Calving-related pulses in velocity are only predicted  
 222 to impact velocity noticeably for the grounded portion of RNK (Figure S2d), and while  
 223 we observe sub-seasonal velocity pulses that are coincident with some of these predicted  
 224 events (blue dashed box in Figures 2m and S2), they have a magnitude that is muted  
 225 compared to those predicted by the terminus-driven model. Further, there are many more  
 226 predicted velocity pulses from large calving events than are visible in the observed ve-  
 227 locity.

228 While both KAN and AVA experience summertime terminus retreat and winter-  
 229 time terminus advance similar to the other three glaciers, their velocity response is poorly  
 230 predicted by the terminus-driven model. For these two glaciers, we observe accelerations  
 231 during winter (during terminus advance) that plateau before the onset of the following  
 232 year's melt season, and early melt season accelerations with the annual maximum ve-  
 233 locity reached in the middle of the melt season (black dashed boxed in Figures 2n, S3,  
 234 and S5). The terminus-driven model does not capture wintertime acceleration because  
 235 the terminus at this time is advancing. For KAN, the model predicts slight deceleration  
 236 in winter (Figure 2n and S5). For AVA, there is no significant seasonality in the simu-  
 237 lated velocity likely because the scale of seasonal terminus advance and retreat for this  
 238 glacier is small (Figure 2o and S3) and the frontal surface elevation is flat (Figure S8).  
 239 The averaged seasonal terminus variation is 144 meters for AVA, while EQP is 224 me-  
 240 ters, KAN is 390 meters, and KUJ is 417 meters.

241 We investigate the influence of changing surface topography by comparing the ve-  
 242 locity simulated using a fixed geometry against velocity simulated using a seasonally vary-  
 243 ing surface elevation from 2018-2022. We find minimal differences between these results  
 244 (blue versus red lines in Figure 2). To investigate this further, we consider only KUJ as  
 245 an example and probe the terminus-driven model via two experiments; 1) we artificially  
 246 shift the entire elevation profile vertically by  $\pm 10$ -20 meters and; 2) we alter the slope  
 247 of the surface elevation by  $\pm 2\%$  within the 2 km-frontal region. The results suggest that  
 248 terminus-driven velocities are relatively insensitive to spatially uniform, along-flow changes  
 249 in surface elevation, but are highly sensitive to changes in surface slope (Figure S9). This  
 250 result is important for providing context for interpreting the results for RNK, which has  
 251 a flat, floating portion of the terminus. We find that the floating region of RNK exhibits  
 252 seasonal variations in velocity of comparable magnitude to the observations in the grounded  
 253 region (Figure S2e). However, the terminus-driven model simulates velocities that have  
 254 no discernible seasonality for the floating region, nor is the magnitude of the simulated  
 255 velocity comparable to what is observed for RNK (Figure S2e).

## 256 4 Discussion

257 Using high-temporal-resolution observations and a terminus-driven model to simu-  
 258 late velocity variations from terminus change, we investigate sub-seasonal velocity changes  
 259 for GrIS outlet glaciers and find that glacier velocity responds to multiple compound-  
 260 ing processes. The seasonal velocity changes of three glaciers (KUJ, EQP, and RNK) can  
 261 largely be attributed to seasonal terminus variation, particularly for KUJ, which has a  
 262 velocity that is almost entirely driven by the terminus fluctuations. However, 4 out of

263 5 study glaciers experience additional processes that drive changes in velocity. For ex-  
 264 ample, EQP, RNK, AVA, and KAN all experience occasional sub-seasonal peaks in ve-  
 265 locity that are coincident with the middle of the melt season, AVA and KAN exhibit win-  
 266 tertime speedup that occurs when their termini are advancing, and RNK experiences short-  
 267 time pulses in velocity throughout the record (Figure 2).

268 The availability of seasonally-resolved elevation change allows us to investigate the  
 269 degree to which velocity is sensitive to changing surface elevation. We find that seasonal  
 270 elevation changes for EQP, KAN, KUJ, and AVA are overall uniform along flow (Fig-  
 271 ure S8), and as a result, they do not significantly alter terminus-driven velocity (blue lines  
 272 in Figures 2, S3-S6). This aligns with our experimental results that suggest that over-  
 273 all vertical shifts in elevation have a limited contribution to velocity seasonality (Figure  
 274 S9a). The experimental results also suggest steepening surface elevation will cause stronger  
 275 velocity responses (Figure S9b), which agrees with our simulation results for RNK that  
 276 seasonality is comparable with observations along the steep grounded flowlines but nearly  
 277 absent on flat floating flowlines (Figure S2).

278 We hypothesize that the peaks in the middle of the melt season observed for EQP,  
 279 RNK, AVA, and KAN (black dashed squares in Figure 2 and Supplementary Figures)  
 280 result from runoff-driven acceleration and subsequent evolution of the subglacial drainage  
 281 system (Moon et al., 2014; Vijay et al., 2019). Early in the melt season, the subglacial  
 282 drainage system is inefficient (Andrews et al., 2014), thus as meltwater availability be-  
 283 gins to increase (marked by increasing runoff in early summer), subglacial water pres-  
 284 sures increase enhancing basal sliding by reducing friction between the ice and the bed  
 285 (Bartholomew et al., 2010; Bartholomäus et al., 2008). As the melt season progresses,  
 286 the drainage system channelizes becoming more efficient (Andrews et al., 2014; Schoof,  
 287 2010) and available meltwater decreases, producing a reduction in glacier speed. After  
 288 the melt season, the impact of terminus retreat on seasonal velocities can become more  
 289 pronounced. For example, EQP typically has a melt season that ends in October, but  
 290 the terminus continues to retreat until December/January (Figure 2l). This produces  
 291 a wintertime peak in velocity that is coincident with the most retreated terminus of EQP  
 292 and is distinct from the melt-season peak.

293 To further explore the velocity variations that are not driven by terminus, we take  
 294 a closer look at the velocity profiles for EQP, KAN, and AVA at particular times in our  
 295 time series (Figure 3). To confirm that runoff drives summertime speed up for EQP, we  
 296 compare the along-flow spatial pattern of velocity changes that occur in the summer melt  
 297 season of 2017 (Apr 2017 - Sep 2017) and the subsequent time period after runoff has  
 298 ceased, when the velocity is primarily influenced by terminus changes (Oct 2017 - Mar  
 299 2018). We quantify the range of upstream velocity at a distance of 8 km upstream of the  
 300 terminus, 20 times the glacier’s frontal thickness from the terminus to ensure we are sev-  
 301 eral longitudinal coupling lengths upstream of the terminus. We find that runoff-driven  
 302 acceleration is noticeable in the velocity further upstream than the terminus-driven ve-  
 303 locity change. For example, when the runoff is large, EQP experiences a range in upstream  
 304 velocity that is 80% of the velocity range observed at the terminus (Figure 3a). Conversely,  
 305 in the winter when runoff is absent and the terminus alone is changing, EQP experiences  
 306 a range in upstream velocity inland that is just 19% of what is observed at the termi-  
 307 nus (Figure 3b). The rapid decline in speed with distance from the terminus is expected  
 308 in the terminus-driven model because of the decline in terminus force with distance from  
 309 the terminus (Joughin et al., 2012), while elevated inland velocities are typical for melt-  
 310 driven acceleration (Sundal et al., 2011) because meltwater percolates throughout the  
 311 ablation zone (Andrews et al., 2014), which extends about 700 km inland of the termi-  
 312 nus for EQP (Noël et al., 2019).

313 AVA and KAN experience mid-summer velocity pulses similar to EQP, suggesting  
 314 these pulses are also likely runoff-driven. However, these two glaciers do not exhibit any  
 315 terminus-driven seasonal acceleration (Figures S3 and S5) and instead accelerate in win-

316 ter. This suggests that seasonal velocity changes for these glaciers occur independent of  
317 terminus change. Similar to melt-driven summertime velocity pulses, we observe that  
318 wintertime speed up for AVA and KAN also extends far inland (Figure 3). For KAN,  
319 we observe that the range in upstream velocity during wintertime speed up is 72% of the  
320 range in frontal velocity. For AVA, we see a smaller range of velocities upstream, where  
321 they are 39% of the range of frontal velocity. However, the range in upstream velocity  
322 remains large compared to EQP and KAN (Figure 3d). We hypothesize that the elevated  
323 range of KAN and AVA's upstream velocities in winter suggests that winter accelera-  
324 tion is due to enhanced extensive basal slip, which can be caused by several different pro-  
325 cesses. During the onset of winter, refreezing of percolating meltwater (Boon & Sharp,  
326 2003) and viscous deformation over subglacial conduits (Vielé et al., 2004; Bartholomäus  
327 et al., 2011) can obstruct the drainage system. Consequently, water becomes trapped  
328 within an inefficient drainage network, leading to increased water pressure and winter  
329 accelerations (Vijay et al., 2019). There are three possible sources of water at the ice-  
330 bed interface during winter: 1) remnants of summer meltwater (Iken & Truffe, 1997),  
331 englacial water stored by basal crevasses that do not reach the surface (Abe & Furuya,  
332 2015; Harper et al., 2010), and sustained exfiltration of underground water caused by  
333 rapid unloading in melt season (Robel et al., 2023). The winter acceleration phase ends  
334 when the melt season begins to supply additional water to the subglacial system, which  
335 further increases basal water pressures causing summertime pulses in speed forcing the  
336 glacier to reach maximum speeds in summer.

337 RNK is a glacier that experiences three distinct modes of velocity variations includ-  
338 ing 1) seasonal terminus-driven velocity change; 2) occasional runoff-driven velocity change  
339 and; 3) frequent, small-magnitude velocity change that appears to be linked to large calv-  
340 ing events. Large calving events have been documented to cause step-like acceleration  
341 for large calving events at Helheim Glacier (Nettles et al., 2008; de Juan et al., 2010) and,  
342 like Helheim, RNK experiences calving via buoyant flexure in which large tabular ice-  
343 bergs detach causing glacier-wide step retreats in the terminus position (Fried et al., 2018;  
344 Medrzycka et al., 2016). Calving-related velocity pulses at RNK are muted compared  
345 to those predicted by the terminus-driven model. In part, this may be due to the lower  
346 sampling frequency of terminus change. Prior to 2017, our terminus record contains just  
347 six termini per month. Indeed, we observe more velocity pulses related to calving events  
348 that are well predicted from the terminus-driven model after 2017, when there are up  
349 to fourteen termini per month. In addition to reduced sampling frequency, the floating  
350 portion of RNK with its flat surface topography likely produces a weaker response to calv-  
351 ing events than would be seen on grounded ice, with its steeper surface topography. This  
352 may additionally explain the muted calving response.

353 For RNK, the velocity changes on the floating flowlines may be driven by lateral  
354 stresses originating on the adjacent grounded ice. The floating portion of the RNK ter-  
355 minus produces simulated velocities that exhibit only minimal change over time (Fig-  
356 ure S2), indicating that velocity change is not driven by terminus variation. In contrast,  
357 the observed velocities in the floating portion of RNK show just as much variation over  
358 time as we observe in the grounded portion. We attribute this discrepancy to the fact  
359 that the terminus-driven model captures longitudinal stresses but not lateral stresses.  
360 Thus, the seasonal variations in the observed velocity over the floating region might be  
361 driven by the nearby velocities on the grounded ice through lateral stress, which is not  
362 captured by the terminus-driven model. The impact of flotation may also be observed  
363 on the grounded ice. For example, in 2017 and 2018 RNK underwent a large multi-year  
364 advance ( $\sim 1000$  meters), after which the seasonal variations in both simulated and ob-  
365 served velocity in the grounded ice are reduced in amplitude compared to other years.  
366 We speculate that as the glacier advanced, its original grounded front became floating  
367 and the surface flattened, which caused the velocity to be less sensitive to seasonal ter-  
368 minus variation.

## 5 Conclusion

We apply a terminus-driven model to elucidate the seasonal and sub-seasonal velocity changes for five glaciers in Central West Greenland. The comparison between simulated and observed velocity suggests that glacier velocity change is driven by the interplay of multiple processes: terminus variations, runoff changes, evolution of the subglacial drainage system, and calving. Notably, the observed seasonal elevation changes appear to have limited influence on velocity largely because the seasonal elevation signal is dominated by shifts in elevation and not changes in surface slope. While the terminus-driven model can effectively isolate the contribution of terminus changes on seasonal velocity variations, several unresolved issues remain. For instance, it is still unclear why some glaciers (RNK, KUJ, and EQP) display sensitivity to terminus changes, while others (KAN and AVA) apparently do not. Our study provides a framework that can be applied to all outlet glaciers around the Greenland Ice Sheet to reveal the compounded nature of each glacier's seasonality. Moreover, the same framework could be applied to investigate the long-term changes in glacier dynamics with adequate historical data. By systematically discerning the commonalities and disparities among glaciers with distinct glaciological settings, our approach has the potential to shed light on the controls on outlet glaciers.

## Acknowledgments

We acknowledge funding for this work from NASA (Grant NNH20ZDA001N-ICESAT2) and the Institute for Geophysics Postdoctoral Fellowship at the Jackson School to E. Zhang. We acknowledge the National Snow and Ice Data Center QGreenland package (Moon et al., 2023). We acknowledge DEMs provided by the Polar Geospatial Center under NSF-OPP awards 1043681, 1559691, 1542736, 1810976, and 2129685.

## References

- Abe, T., & Furuya, M. (2015). Winter speed-up of quiescent surge-type glaciers in Yukon, Canada. *The Cryosphere*, 9(3), 1183–1190. doi: 10.5194/tc-9-1183-2015
- Andrews, L. C., Catania, G. A., Hoffman, M. J., Gulley, J. D., Lüthi, M. P., Ryser, C., . . . Neumann, T. A. (2014). Direct observations of evolving subglacial drainage beneath the Greenland ice sheet. *Nature*, 514(7520), 80–83. doi: 10.1038/nature13796
- Bartholomäus, T. C., Anderson, R. S., & Anderson, S. P. (2008). Response of glacier basal motion to transient water storage. *Nature Geoscience*, 1(1), 33–37. doi: 10.1038/ngeo.2007.52
- Bartholomäus, T. C., Anderson, R. S., & Anderson, S. P. (2011). Growth and collapse of the distributed subglacial hydrologic system of Kennicott glacier, Alaska, USA, and its effects on basal motion. *Journal of Glaciology*, 57(206), 985–1002. doi: 10.3189/002214311798843269
- Bartholomew, I., Nienow, P., Mair, D., Hubbard, A., King, M. A., & Sole, A. (2010). Seasonal evolution of subglacial drainage and acceleration in a Greenland outlet glacier. *Nature Geoscience*, 3(6), 408–411. doi: 10.1038/ngeo863
- Boon, S., & Sharp, M. (2003). The role of hydrologically-driven ice fracture in drainage system evolution on an Arctic glacier. *Geophysical Research Letters*, 30(18). doi: https://doi.org/10.1029/2003GL018034
- Catania, G. A., Stearns, L. A., Sutherland, D. A., Fried, M. J., Bartholomäus, T. C., Morlighem, M., . . . Nash, J. (2018). Geometric controls on tidewater glacier retreat in central western Greenland. *Journal of Geophysical Research: Earth Surface*, 123(8), 2024–2038. doi: 10.1029/2017JF004499
- Davison, B. J., Sole, A. J., Cowton, T. R., Lea, J. M., Slater, D. A., Fahrner, D., & Nienow, P. W. (2020). Subglacial drainage evolution modulates seasonal

- ice flow variability of three tidewater glaciers in southwest greenland. *Journal of Geophysical Research: Earth Surface*, 125(9), e2019JF005492. doi: <https://doi.org/10.1029/2019JF005492>
- de Juan, J., Elósegui, P., Nettles, M., Larsen, T. B., Davis, J. L., Hamilton, G. S., ... Forsberg, R. (2010). Sudden increase in tidal response linked to calving and acceleration at a large greenland outlet glacier. *Geophysical Research Letters*, 37(12), L12501. doi: <https://doi.org/10.1029/2010GL043289>
- Enderlin, E. M., Howat, I. M., Jeong, S., Noh, M.-J., van Angelen, J. H., & van den Broeke, M. R. (2014). An improved mass budget for the Greenland ice sheet. *Geophysical Research Letters*, 41(3), 866-872. doi: 10.1002/2013GL059010
- Felikson, D., A. Catania, G., Bartholomäus, T. C., Morlighem, M., & Noël, B. P. Y. (2021). Steep glacier bed knickpoints mitigate inland thinning in greenland. *Geophysical Research Letters*, 48(2), e2020GL090112. doi: <https://doi.org/10.1029/2020GL090112>
- Felikson, D., Nowicki, S., Nias, I., Morlighem, M., & Seroussi, H. (2022). Seasonal tidewater glacier terminus oscillations bias multi-decadal projections of ice mass change. *Journal of Geophysical Research: Earth Surface*, 127(2), e2021JF006249. doi: <https://doi.org/10.1029/2021JF006249>
- Fried, M. J., Catania, G. A., Stearns, L. A., Sutherland, D. A., Bartholomäus, T. C., Shroyer, E., & Nash, J. (2018). Reconciling Drivers of Seasonal Terminus Advance and Retreat at 13 Central West Greenland Tidewater Glaciers. *Journal of Geophysical Research: Earth Surface*, 123(7), 1590-1607. doi: 10.1029/2018JF004628
- Gardner, A. S., Fahnestock, M. A., & Scambos, T. A. (2023). *ITS\_LIVE regional glacier and ice sheet surface velocities: Version 1*. National Snow and Ice Data Center. Retrieved from <https://doi:10.5067/6II6VW8LLWJ7>
- Gardner, A. S., Moholdt, G., Scambos, T., Fahnestock, M., Ligtenberg, S., van den Broeke, M., & Nilsson, J. (2018). Increased west antarctic and unchanged east antarctic ice discharge over the last 7 years. *The Cryosphere*, 12(2), 521-547. doi: 10.5194/tc-12-521-2018
- Goliber, S., Black, T., Catania, G., Lea, J. M., Olsen, H., Cheng, D., ... Zhang, E. (2022). Termpicks: a century of greenland glacier terminus data for use in scientific and machine learning applications. *The Cryosphere*, 16(8), 3215-3233. doi: 10.5194/tc-16-3215-2022
- Harper, J. T., Bradford, J. H., Humphrey, N. F., & Meierbachtol, T. W. (2010). Vertical extension of the subglacial drainage system into basal crevasses. *Nature*, 467(7315), 579-582. doi: 10.1038/nature09398
- Holland, D. M., Thomas, R. H., De Young, B., Ribergaard, M. H., & Lyberth, B. (2008). Acceleration of Jakobshavn Isbræ triggered by warm subsurface ocean waters. *Nature geoscience*, 1(10), 659-664. doi: 10.1038/ngeo316
- Howat, I. M., Joughin, I., Fahnestock, M., Smith, B. E., & Scambos, T. A. (2008). Synchronous retreat and acceleration of southeast Greenland outlet glaciers 2000-06: ice dynamics and coupling to climate. *Journal of Glaciology*, 54(187), 646-660. doi: 10.3189/002214308786570908
- Howat, I. M., Joughin, I., Tulaczyk, S., & Gogineni, S. (2005). Rapid retreat and acceleration of Helheim Glacier, east Greenland. *Geophysical Research Letters*, 32(22), L22502. doi: 10.1029/2005GL024737
- Iken, A., & Truffe, M. (1997). The relationship between subglacial water pressure and velocity of findelengletscher, switzerland, during its advance and retreat. *Journal of Glaciology*, 43(144), 328-338. doi: 10.3189/S0022143000003282
- IPCC. (2022). *Climate change 2022: Mitigation of climate change* (P. Shukla et al., Eds.). Cambridge, UK and New York, NY, USA: Cambridge University Press. doi: 10.1017/9781009157926
- Joughin, I., Das, S. B., King, M. A., Smith, B. E., Howat, I. M., & Moon, T. (2008). Seasonal Speedup Along the Western Flank of the Greenland Ice Sheet. *Sci-*

- ence, *320*(5877), 781–783. doi: 10.1126/science.1153288
- 476 Joughin, I., Smith, B. E., Howat, I. M., Floricioiu, D., Alley, R. B., Truffer, M., &  
477 Fahnestock, M. (2012). Seasonal to decadal scale variations in the surface  
478 velocity of Jakobshavn Isbrae, Greenland: Observation and model-based anal-  
479 ysis. *Journal of Geophysical Research: Earth Surface*, *117*(F2), F02030. doi:  
480 10.1029/2011JF002110
- 481 Kehrl, L. M., Joughin, I., Shean, D. E., Floricioiu, D., & Krieger, L. (2017). Sea-  
482 sonal and interannual variabilities in terminus position, glacier velocity, and  
483 surface elevation at Helheim and Kangerlussuaq Glaciers from 2008 to 2016.  
484 *Journal of Geophysical Research: Earth Surface*, *122*(9), 1635-1652. doi:  
485 10.1002/2016JF004133
- 486 King, M. D., Howat, I. M., Candela, S. G., Noh, M. J., Jeong, S., Noël, B. P., ...  
487 Negrete, A. (2020). Dynamic ice loss from the greenland ice sheet driven by  
488 sustained glacier retreat. *Communications Earth & Environment*, *1*(1), 1. doi:  
489 10.1038/s43247-020-0001-2
- 490 Medley, B., Neumann, T. A., Zwally, H. J., Smith, B. E., & Stevens, C. M. (2022).  
491 Simulations of firn processes over the greenland and antarctic ice sheets: 1980–  
492 2021. *The Cryosphere*, *16*(10), 3971–4011. doi: 10.5194/tc-16-3971-2022
- 493 Medrzycka, D., Benn, D. I., Box, J. E., Copland, L., & Balog, J. (2016). Calving be-  
494 havior at rink isbræ, west greenland, from time-lapse photos. *Arctic, Antarctic,  
495 and Alpine Research*, *48*(2), 263-277. doi: 10.1657/AAAR0015-059
- 496 Moon, T., Fisher, M., Stafford, T., & Thurber, A. (2023). *Qgreenland (v3) [dataset]*.  
497 National Snow and Ice Data Center. Retrieved from [https://10.5281/zenodo](https://10.5281/zenodo.8326507)  
498 [.8326507](https://10.5281/zenodo.8326507)
- 499 Moon, T., Gardner, A., Csatho, B., Parmuzin, I., & Fahnestock, M. (2020). Rapid  
500 Reconfiguration of the Greenland Ice Sheet Coastal Margin. *Journal of Geo-*  
501 *physical Research: Earth Surface*, *125*(11). doi: 10.1029/2020jf005585
- 502 Moon, T., Joughin, I., & Smith, B. (2015). Seasonal to multiyear variability of  
503 glacier surface velocity, terminus position, and sea ice/ice mélange in northwest  
504 Greenland. *Journal of Geophysical Research: Earth Surface*, *120*(5), 818-833.  
505 doi: 10.1002/2015JF003494
- 506 Moon, T., Joughin, I., Smith, B., & Howat, I. (2012). 21st-Century evolution of  
507 Greenland outlet glacier velocities. *Science*, *336*(6081), 576–578. doi: 10.1126/  
508 science.1219985
- 509 Moon, T., Joughin, I., Smith, B., van den Broeke, M. R., van de Berg, W. J.,  
510 Noël, B., & Usher, M. (2014). Distinct patterns of seasonal Greenland  
511 glacier velocity. *Geophysical Research Letters*, *41*(20), 7209-7216. doi:  
512 10.1002/2014GL061836
- 513 Morlighem, M., Williams, C. N., Rignot, E., An, L., Arndt, J. E., Bamber, J. L.,  
514 ... Zinglarsen, K. B. (2017). BedMachine v3: Complete bed topography  
515 and ocean bathymetry mapping of Greenland from multibeam echo dound-  
516 ing combined with mass conservation. *Geophysical Research Letters*, *44*(21),  
517 11,051-11,061. doi: 10.1002/2017GL074954
- 518 Morlighem, M., Williams, C. N., Rignot, E., An, L., Arndt, J. E., Bamber, J. L.,  
519 ... Zinglarsen, K. B. (2022). *Icebridge bedmachine greenland, version 5 [data*  
520 *set]*. Boulder, Colorado USA. NASA National Snow and Ice Data Center Dis-  
521 tributed Active Archive Center. Retrieved from [https://doi.org/10.5067/](https://doi.org/10.5067/GMEVBWFLWA7X)  
522 [GMEVBWFLWA7X](https://doi.org/10.5067/GMEVBWFLWA7X). DateAccessed08-30-2023.
- 523 Nettles, M., Larsen, T. B., Elósegui, P., Hamilton, G. S., Stearns, L. A., Ahlstrøm,  
524 A. P., ... Forsberg, R. (2008). Step-wise changes in glacier flow speed co-  
525 incide with calving and glacial earthquakes at helheim glacier, greenland.  
526 *Geophysical Research Letters*, *35*(24), L24503. doi: [https://doi.org/10.1029/](https://doi.org/10.1029/2008GL036127)  
527 [2008GL036127](https://doi.org/10.1029/2008GL036127)
- 528 Noël, B., van de Berg, W. J., Lhermitte, S., & van den Broeke, M. R. (2019). Rapid  
529 ablation zone expansion amplifies north greenland mass loss. *Science Ad-*

- 530 *vances*, 5(9), eaaw0123. doi: 10.1126/sciadv.aaw0123
- 531 Porter, C., Morin, P., Howat, I. M., Noh, M.-J., Bates, B., Peterman, K., ... Bo-  
532 jesen, M. (2022). *ArcticDEM - Strips, Version 4.1*. Retrieved 2023, from  
533 <https://doi.org/10.7910/DVN/C98DVS>
- 534 Rennermalm, A. K., Smith, L. C., Chu, V. W., Box, J. E., Forster, R. R., Van den  
535 Broeke, M. R., ... Moustafa, S. E. (2013). Evidence of meltwater reten-  
536 tion within the greenland ice sheet. *The Cryosphere*, 7(5), 1433–1445. doi:  
537 10.5194/tc-7-1433-2013
- 538 Robel, A. A., Sim, S. J., Meyer, C., Siegfried, M. R., & Gustafson, C. D. (2023).  
539 Contemporary ice sheet thinning drives subglacial groundwater exfiltration  
540 with potential feedbacks on glacier flow. *Science Advances*, 9(33), eadh3693.  
541 doi: 10.1126/sciadv.adh3693
- 542 Schoof, C. G. (2010, 12). Ice-sheet acceleration driven by melt supply variability.  
543 *Nature*, 468(7325), 803–806. doi: 10.1038/nature09618
- 544 Shepherd, A., Ivins, E. R., A, G., Barletta, V. R., Bentley, M. J., Bettadpur, S., ...  
545 Zwally, H. J. (2012). A reconciled estimate of ice-sheet mass balance. *Science*,  
546 338(6111), 1183–1189. doi: 10.1126/science.1228102
- 547 Solgaard, A. M., Rapp, D., Noël, B. P. Y., & Hvidberg, C. S. (2022). Sea-  
548 sonal patterns of greenland ice velocity from sentinel-1 sar data linked  
549 to runoff. *Geophysical Research Letters*, 49(24), e2022GL100343. doi:  
550 <https://doi.org/10.1029/2022GL100343>
- 551 Stevens, L. A., Nettles, M., Davis, J. L., Creyts, T. T., Kingslake, J., Hewitt,  
552 I. J., & Stubblefield, A. (2022). Tidewater-glacier response to supraglacial  
553 lake drainage. *Nature Communications*, 13(1), 6065. doi: 10.1038/  
554 s41467-022-33763-2
- 555 Sundal, A. V., Shepherd, A., Nienow, P., Hanna, E., Palmer, S., & Huybrechts,  
556 P. (2011). Melt-induced speed-up of greenland ice sheet offset by efficient  
557 subglacial drainage. *Nature*, 469(7331), 521–524. doi: 10.1038/nature09740
- 558 Ultee, L., Felikson, D., Minchew, B., Stearns, L. A., & Riel, B. (2022). Hel-  
559 heim glacier ice velocity variability responds to runoff and terminus position  
560 change at different timescales. *Nature Communications*, 13(1), 6022. doi:  
561 10.1038/s41467-022-33292-y
- 562 van den Broeke, M. R., Enderlin, E. M., Howat, I. M., Kuipers Munneke, P., Noël,  
563 B. P. Y., van de Berg, W. J., ... Wouters, B. (2016). On the recent contri-  
564 bution of the greenland ice sheet to sea level change. *The Cryosphere*, 10(5),  
565 1933–1946. doi: 10.5194/tc-10-1933-2016
- 566 Van der Veen, C. J. (2013). *Fundamentals of glacier dynamics* (Second Edition ed.).  
567 New York: CRC press.
- 568 Vieli, A., Jania, J., Blatter, H., & Funk, M. (2004). Short-term velocity varia-  
569 tions on hansbreen, a tidewater glacier in spitsbergen. *Journal of Glaciology*,  
570 50(170), 389–398. doi: 10.3189/172756504781829963
- 571 Vijay, S., Khan, S. A., Kusk, A., Solgaard, A. M., Moon, T., & Bjørk, A. A.  
572 (2019). Resolving seasonal ice velocity of 45 greenlandic glaciers with very  
573 high temporal details. *Geophysical Research Letters*, 46(3), 1485–1495. doi:  
574 <https://doi.org/10.1029/2018GL081503>
- 575 Vijay, S., King, M. D., Howat, I. M., Solgaard, A. M., Khan, S. A., & Noël, B.  
576 (2021). Greenland ice-sheet wide glacier classification based on two distinct  
577 seasonal ice velocity behaviors. *Journal of Glaciology*, 67(266), 1241–1248. doi:  
578 10.1017/jog.2021.89
- 579 Werder, M. A., Hewitt, I. J., Schoof, C. G., & Flowers, G. E. (2013). Modeling chan-  
580 nelerized and distributed subglacial drainage in two dimensions. *Journal of Geo-*  
581 *physical Research: Earth Surface*, 118(4), 2140–2158. doi: [https://doi.org/10](https://doi.org/10.1002/jgrf.20146)  
582 [.1002/jgrf.20146](https://doi.org/10.1002/jgrf.20146)
- 583 Wood, M., Rignot, E., Fenty, I., An, L., Bjørk, A., van den Broeke, M., ... others  
584 (2021). Ocean forcing drives glacier retreat in greenland. *Science Advances*,

585 7(1), eaba7282. doi: 10.1126/sciadv.aba7282  
586 Zhang, E., Catania, G., & Trugman, D. T. (2023). Autoterm: an automated pipeline  
587 for glacier terminus extraction using machine learning and a “big data” repos-  
588 itory of greenland glacier termini. *The Cryosphere*, 17(8), 3485–3503. doi:  
589 10.5194/tc-17-3485-2023

## 590 **Open Research Section**

591 Velocity data can be freely downloaded at <https://its-live.jpl.nasa.gov/> (Gardner  
592 et al., 2023). ArcticDEMs are available at <https://livingatlas2.arcgis.com/arcticdemexplorer/>.  
593 The code, terminus data, flowlines, and DG-IS2-DEMs can be downloaded at [https://](https://zenodo.org/record/8428196)  
594 [zenodo.org/record/8428196](https://zenodo.org/record/8428196).

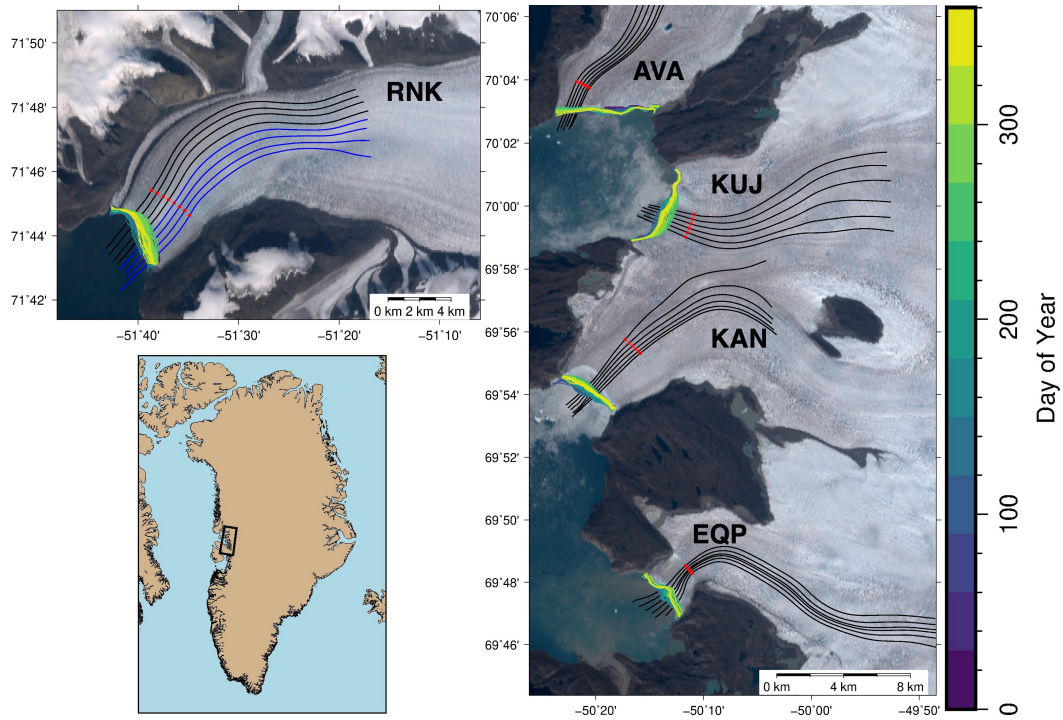


**Figure 1.** Glacier and data locations. Glaciers examined in this study include Rink Isbrae (RNK), Sermeq Avannarleq (AVA), Sermeq Kujalleq (KUJ), Kangilernata Sermia (KAN), and Eqip Sermia (EQP). Black flowlines represent grounded portions of the glaciers while blue flowlines represent floating portions of the glaciers. The terminus traces in 2018 from AutoTerm are colored by date. Red points on each flowline are the locations where we obtain velocity time series from ITS\_LIVE.

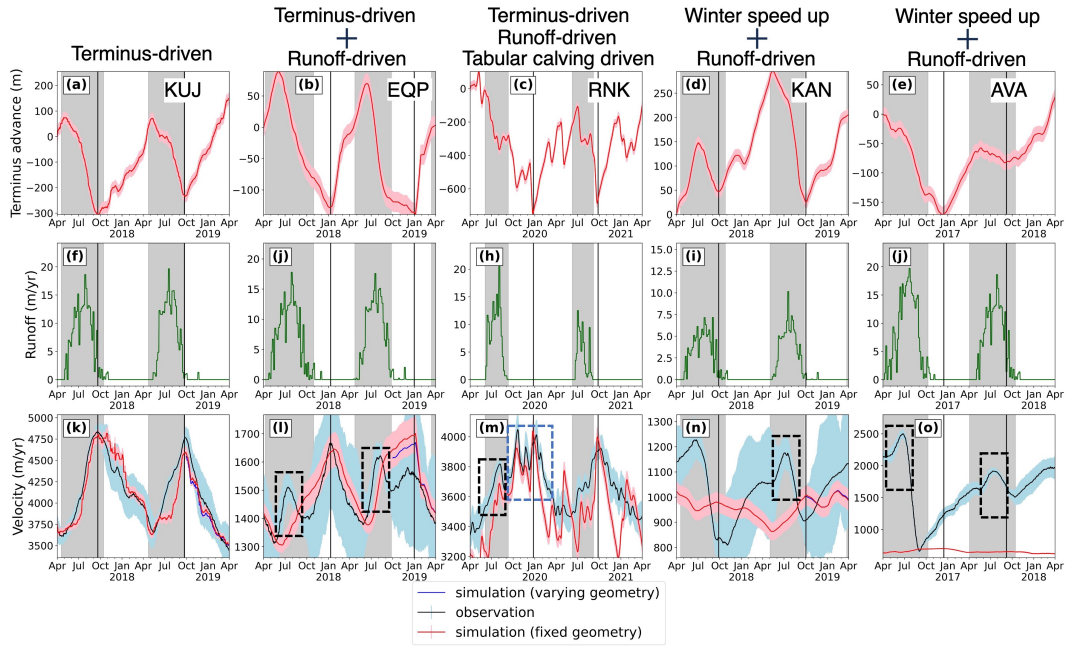


**Figure 2.** Comparison between velocity observations and simulations and examples of compounded seasonality. The left column is the results of KUJ, the middle column is for EQP, the third column is for RNK, the fourth column is for KAN, and the fifth column is for AVA. The black vertical lines indicate the end of retreating. The shaded areas indicated melt seasons. The blue-shaded areas indicate the uncertainty of the velocity observations, and the pink-shaded areas indicate the terminus uncertainty. The dashed boxes show the acceleration induced by runoff. The blue dashed box in (m) shows the acceleration caused by large calving events.

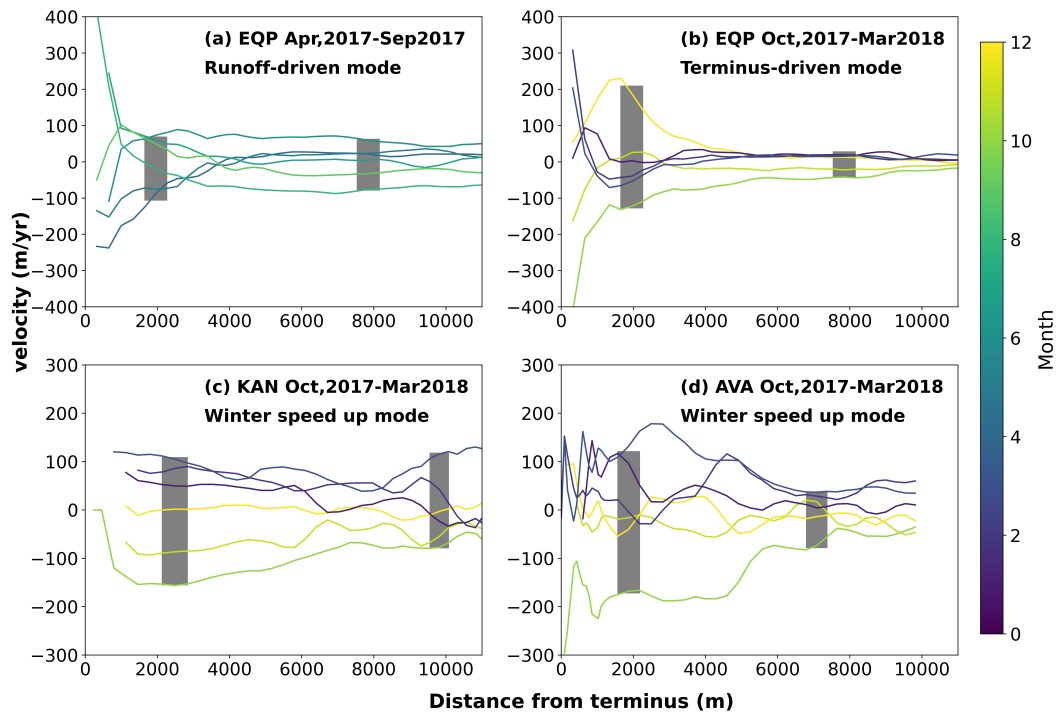


**Figure 3.** Velocity profiles over time for EQP, KAN, and AVA. The average velocity profile has been subtracted for a better display of changes over time. The original velocity profiles are shown in Figure S10. The shaded areas indicate regions where we obtain velocity variations in the frontal and upstream sections. (a) Velocity profiles of EQP during the melt season. (b) Velocity profiles of EQP after the melt season, during which velocity is primarily influenced by terminus changes. (c) Velocity profile of KAN during winter and early melt season. (d) Velocity profile of AVA during winter and early melt season.